Detection and variability of TiO_2 using LROC WAC UVVIS data at calibration sites. E. O. Coman[1] and B. L. Jolliff[1], [1]Department of Earth and Planetary Sciences, Washington University in St. Louis, One Brookings Drive, St. Louis, MO 63130, ecoman@wustl.edu

Introduction: Lunar remote sensing at ultraviolet (UV) and visible (VIS) wavelengths reveals a range of compositional differences across the lunar surface. Notably, a UV/VIS spectral ratio correlates well with TiO_2 likely owing to the flat reflectance spectra of ilmenite, the main carrier of TiO_2 on the lunar surface [1-14]. UV/VIS spectral ratios derived from Hubble Telescope (502/250) and Lunar Reconnaissance Orbiter Camera (LROC) Wide Angle Camera (WAC) (321/415) have shown less sensitivity to maturity variations than spectral ratios formed from only visible (400-750 nm) wavelengths [8,15]. The LROC WAC is the only lunar orbiting spectrometer with bands at these ultraviolet wavelengths.

The wide range of TiO_2 concentrations (0 to >14 wt.%) on the lunar surface have made this oxide of particular importance for understanding lunar volcanic history and evolution; improved detection methods can delineate mare basalt heterogeneities and composition, improving our knowledge of lunar volcanism and the source regions that formed these various basalts [16]. To better understand the current titanium detection algorithms, we analyze and compare the results of the global LROC WAC TiO_2 (WAC TiO_2) to Clementine UVVIS TiO_2 (CL TiO_2) values at the Chang'e-3, Apollo 17, and Apollo 11 landing sites. These regions of interest are chosen for their importance to lunar science, variation in mare basalt TiO_2 concentrations, and available calibration data.

Methods: Data was cropped and resampled to 200 × 200 km regions from the WAC albedo basemap [17], Clementine 5 band warped mosaic [18,19], and LOLA/SELENE merged DEM [20] to 400 mpp and map projected to equirectangular projection to match the photometrically corrected WAC basemap [17]. We calculated CL TiO_2 and WAC TiO_2 algorithms from [21] and [22], respectively.

Results and Discussion

Imbrium at Chang'e-3 site. This location contains younger, high-Ti mare basalt flows overprinting older, low-Ti mare basalts (Fig. 1, regions 1 and 3). We masked out albedos and elevations greater than one standard deviation to avoid slopes and fresh crater ejecta, which may affect TiO_2 calculations. The area shows evidence of mixing (Fig. 1, region 2) between these high- and low-Ti mare regions along flow boundaries and on crater ejecta rings which excavated underlying low-Ti basalts. Chang'e-3 APXS measurements characterize the landing site as an intermediate TiO_2 (~5.0 wt.%) basalt [23], consistent with the specific CL (4.9 wt%) and WAC (6.6 wt%) TiO_2 pixel values corresponding to the landing site. Outside of the Chang'e-3 landing site vicinity, both CL TiO_2 and WAC TiO_2 show higher TiO_2 values than the landing site; the high-Ti lava flow has an average ~7.5 wt.% WAC TiO_2. These findings support the possibility that the Chang'e-3 APXS took measurements in an area where mixing of regolith has occurred between low-Ti material from the northeast and the local high-Ti basalt flow in the southwest.

The WAC TiO_2 and CL TiO_2 values generally fall along a 1-1 line, though WAC TiO_2 is on average higher than CL TiO_2 (Figure 1, inset). This relationship differs from comparisons of global WAC and CL TiO_2 where the WAC typically shows lower TiO_2 values than Clementine [14].

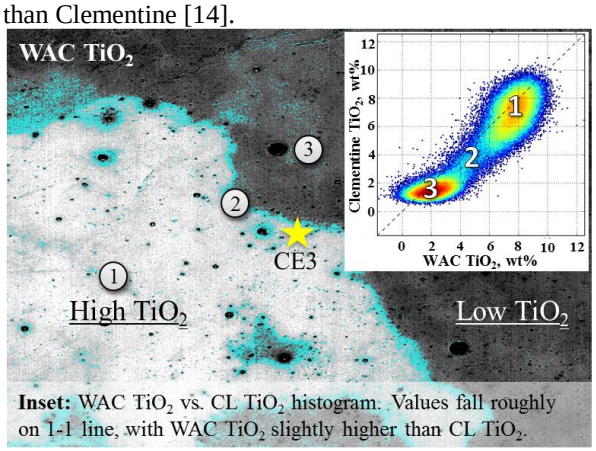

Figure 1. WAC TiO_2 image centered at Chang'e-3 landing site. Brighter pixels correspond to higher TiO_2 flows, darker pixels to lower TiO_2 flows. Cyan areas represent intermediate WAC TiO_2 concentrations (4-6 wt.%).

Apollo 17 site at Taurus Littrow. The Apollo 17 landing site lies on a mare region surrounded by massifs and higher elevation highlands. This area has large albedo and elevation differences, thus we chose to mask regions with albedos and elevations outside the average Apollo 17 landing-site values. Most of the WAC and CL TiO_2 data plot on the 1-1 line with one separate high CL TiO_2 lobe corresponding to a mare basalt region southwest of Taurus Littrow (Fig. 2, region 1). The good fit for the low- and intermediate-TiO_2 dataset can be attributed to the use of well-correlated Apollo-era regolith samples from this

location in the calibration of the TiO_2 detection algorithms.

Low TiO_2 regions (Fig. 2, region 3) fall along the edges of massifs, crater walls, and highlands regions. These areas likely represent downslope mixing of low TiO_2 materials with the high TiO_2 mare basalts below.

The high TiO_2 lobe (region 1) occurs spatially along a bright blue area in the southwest of the Clementine color ratio image (Fig. 2). Low and medium TiO_2 lobes fall along orange and blue areas representative of iron-rich basalts with varying contents of TiO_2 [24, 25].

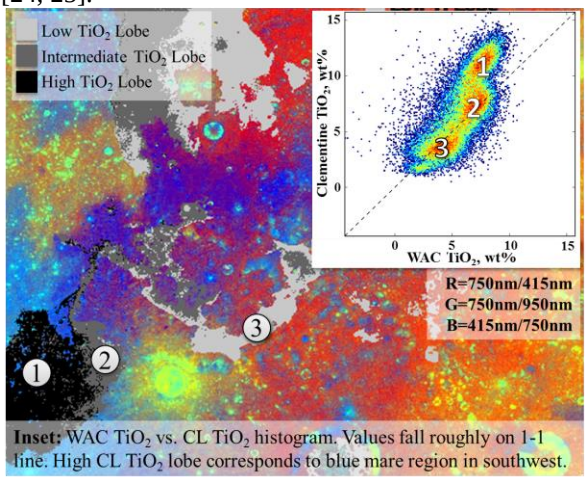

Figure 2. Clementine color ratio of the Taurus Littrow valley centered on Apollo 17.

Tranquillitatis near Apollo 11. Tranquillitatis near the Apollo 11 landing site spans an area of more uniform elevation and albedo than the Taurus Littrow valley. The Clementine color ratio image shows similar composition to the southwestern mare basalts of Taurus Littrow (Fig. 2,3), consistent with the 2D histogram for Tranquillitatis plotting off the 1-1 line owing to higher average TiO_2 values for CL than for WAC. The Apollo 11 point plots as an outlier in the calibration of [21], resulting in the anomalous high CP TiO_2 values at this location.

Conclusions: The basaltic regolith composition at the Chang'e-3 landing site represents a mixture of younger, high-Ti basalt flows and older, low-Ti flows. Comparisons between CL TiO_2 and WAC TiO_2 show a 1-1 correlation at the Apollo 17 and Chang'e-3 landing sites, and can distinguish between various mare regions and mixing trends.

Future work involves improving upon these preliminary results by completing studies of 7 additional areas of interest, most of which are international science coordination and calibration targets as described by [26].

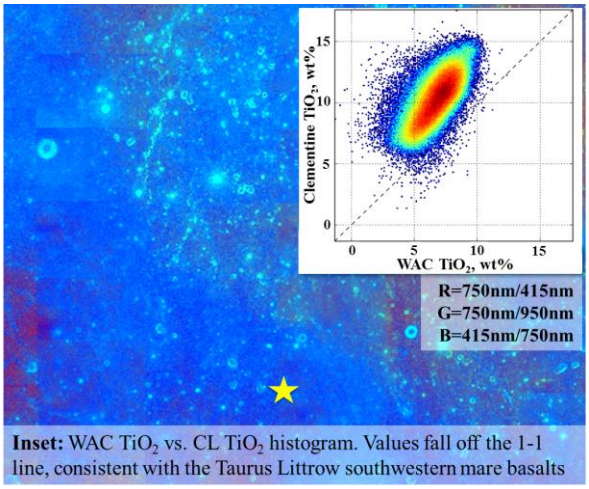

Figure 3. Clementine color ratio of Apollo 11 region (gold star) with stretch equivalent to Fig. 2.

References: [1] Charette M.P. et al. (1974) *JGR, 79*, 1605-1613; [2] Johnson J. et al. (1991), *JGR, 96*, 18861-18882; [3] Johnson J.R. et al. (1991) *GRL, 18*, 2153-2156; [4] Blewett D.T. et al. (1997) *JGR, 102*, 16319-16325; [5] Lucey P.G. et al. (1998) *JGR, 103*, 3679-3699; [6] Gillis J.J. et al. (2003) *JGR, 108*, 5009; [7] Gillis-Davis J.J. et al. (2006) *GCA, 70*, 6079-6102; [8] Robinson M.S. et al. (2007) *GRL, 34*; [9] Robinson M.S. et al. (2011) *LPS 42*, #1842; [10] Sato H. et al. (2015) *LPS 46*, #1111;[11] Cloutis E.A. (2010) *LPS 41*, #1139; [12] Wagner J.K. et al. (1987) *Icarus, 69*, 14-28; [13] Wells E. and Hapke B. (1977) *Science*, 195, 977-99; [14] Sato H. et al. (2015) *LPS*, 46, Abstract #1111. [15] Denevi B.W. et al. (2014) *JGR, 119*, 976-997; [16] Shearer, C.K. et al. (2006) *RMG., 60*, 365-518. [17] Sato H. et al. (2014) *JGR, 119*, 1775-1805. [18] Eliason E.C. et al. (1999) *PDS*, 4001-4078. [19] Hare T.M. et al. (2008) *LPSC 39*, Abstract #2337. [20] Barker M.K. (2016) *Icarus, 273*, 346-355. [21] Lucey P.G. et al. (2000) *JGR, 105*, 20297-20305. [22] Sato H. et al., *Icarus*, submitted. [23] Ling Z. et al. (2015) *NC*, 8880. [24] McEwen A. S. et al (1994) *Science*, 266, 1858-1862. [25] Pieters C. M. et al. (1993) *JGR*, 98, 17127-17148. [26] Pieters C.M. et al. (2008) *ASR, 42*, 248-258.

Acknowledgement: This research used the USGS Integrated Software for Imagers and Spectrometers (ISIS). We appreciate the support of the LRO Project and LROC.